ELSEVIER

Carbohydrate Research 278 (1995) 239–256

CARBOHYDRATE RESEARCH

Multinuclear magnetic resonance studies of the interaction of inorganic cations with heparin

Dallas L. Rabenstein *, Jan M. Robert [1], Jie Peng

Department of Chemistry, University of California, Riverside, CA 92521, USA

Received 14 June 1995; accepted 17 July 1995

Abstract

The interaction of Na^+, Ca^{2+}, Mg^{2+}, Zn^{2+} and La^{3+} with heparin, a highly negatively charged glycosaminoglycan, was studied by ^1H and ^{23}Na nuclear magnetic resonance spectroscopy. ^1H chemical shift and nuclear Overhauser effect (NOE) data indicate that the counter ions Na^+, Ca^{2+} and Mg^{2+} interact with the low pH, carboxylic acid form of heparin by delocalized, long-range electrostatic interactions. At higher pH, ^1H chemical shift and NOE data indicate that Na^+ and Mg^{2+} continue to interact with heparin in the same manner, even upon deprotonation of the carboxylic acid group; however, there is a site-specific contribution to the binding of Ca^{2+}, Zn^{2+} and La^{3+} under these conditions. Acid dissociation constants for heparin carboxylic acid groups and heparin–metal binding constants were determined from the pH dependence of ^1H chemical shifts and ^{23}Na spin-lattice (T_1) relaxation times. Equilibrium constants for exchange of M^{2+} for heparin-bound Na^+ were obtained from ^{23}Na T_1 data. The acid dissociation constants show a strong dependence on Na^+ concentration due to the polyelectrolyte character of heparin.

Keywords: Heparin; ^1H NMR spectroscopy; ^{23}Na NMR spectroscopy; Relaxation times; Conformation; Heparin–metal binding

1. Introduction

Heparin is a highly negatively charged glycosaminoglycan found in small quantities in many mammalian tissues [1]. The structure of heparin is largely accounted for by repeating sequences of the trisulfated disaccharide {(1 → 4)-2-*O*-sulfo-α-L-idopyranosyl-

* Corresponding author.

[1] Present address: Department of Chemistry, University of South Florida, Tampa, FL 33620, USA.

0008-6215/95/$09.50 © 1995 Elsevier Science Ltd. All rights reserved
SSDI 0008-6215(95)00263-4

uronic acid-(1 → 4)-2-deoxy-6-*O*-sulfo-2-sulfoamino-α-D-glucopyranose}.
For example, this repeating disaccharide accounts for at least 85% of heparins from

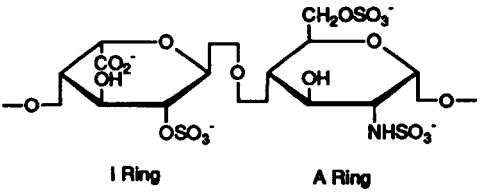

beef lung and 75% of those from intestinal mucosa [2–5]. Minor constituents, including β-D-glucopyranosyluronic acid and 2-acetamido-2-deoxy-6-*O*-sulfo-α-D-glucopyranosyl residues, are present in varying amounts, depending on the source of the heparin.

Heparin is widely used in medicine as an anticoagulant and antithrombotic. Heparin also activates lipoprotein lipase and inhibits the growth and replication of the human immunodeficiency virus (HIV) [5–12]. The activity of heparin can be modulated by Ca^{2+}. For example, Ca^{2+} moderates the anticoagulant activity of heparin [13], it affects heparin-stabilized tryptase in human mast cells [14], it potentiates the acceleration by heparin of thrombin inhibition by antithrombin III and the anti-Factor Xa activity of heparin [15a,b], and it increases the heparin stimulatory effect on the activation of human plasminogen by tissue-type Pg activator [16]. Although the mechanisms by which calcium ions modulate the activities of heparin are not known, it seems likely that Ca^{2+} binding is involved since heparin has a relatively high affinity for Ca^{2+} [17,18]. Also, when used as an anticoagulant, heparin is most likely present in blood plasma as a mixed heparin/Na^+/Ca^{2+} complex since Ca^{2+} is ~2 mM in plasma [19]. Although the interaction of heparin with Ca^{2+} and other metal ions, including Mg^{2+}, Zn^{2+} and Cu^{2+}, has been the subject of numerous studies [17,18,20–36], there is not uniform agreement on the nature of the binding interaction involved. Because of its high negative charge density, heparin is a polyelectrolyte, i.e., a fraction of its negative charge is neutralized by bound counterions [5,17,18,35–41]. Counterions can bind site specifically or territorially to polyelectrolytes [42,43]. In the counterion condensation model of territorial (or delocalized) binding developed by Manning, the bound counterions are in the fully hydrated state characteristic of a purely aqueous environment, they are contained in a cylindrical condensation volume around the polyelectrolyte, and they have unrestricted freedom of motion along the length of the polyelectrolyte within the condensation volume [42,43]. Delocalized binding involves only long-range electrostatic interactions between counterions and ionic sites on the polyelectrolyte.

On the basis of relative binding affinities, it was concluded that both Mg^{2+} and Ca^{2+} interact with heparin by nonspecific electrostatic binding rather than by a site-specific, chelating-type of interaction [22]. However, CD measurements were interpreted to indicate that bound Ca^{2+} neutralizes carboxylate groups preferentially [40]. Perlin and co-workers concluded from NMR studies that Ca^{2+} forms a 1:1 complex with the repeating disaccharide unit, with site specific binding to the carboxylate group and secondary stabilization by binding to the sulfamino group of the next residue [26]. Later,

they reversed these conclusions on the basis of an analysis of ^{13}C chemical shift displacements in terms of Manning's counterion condensation model, which they interpreted to indicate that binding of Ca^{2+} and Mg^{2+} by heparin is a delocalized process involving relatively long-range electrostatic interactions [35,36]. Perlin and co-workers also found that Ca^{2+} does not interact with *N*-desulfated heparin, whereas the modified heparin formed by selective removal of the 2-*O*-sulfo group of the I-ring has the capacity to bind Ca^{2+} despite its reduced overall charge [20]. Mattai and Kwak concluded from an analysis of the extent of binding of Ca^{2+}, Mg^{2+} and Zn^{2+} by heparin in terms of Manning's counterion condensation model that binding of Mg^{2+} is delocalized whereas Ca^{2+} and Zn^{2+} binding is site-specific, with binding constants of 10^2–10^5 M^{-1} at low ionic strengths [17,18].

In this paper, we report the results of ^1H and ^{23}Na NMR studies of the interaction of Na^+, Ca^{2+}, Mg^{2+}, Zn^{2+} and La^{3+} with heparin. Acid dissociation constants for the carboxylic acid group and heparin–metal binding constants were determined from ^1H chemical shift vs. pH titration curves for the heparin/Na^+ and mixed ion (heparin/Na^+/M^{n+} where M^{n+} is Ca^{2+}, Mg^{2+}, Zn^{2+} or La^{3+}) systems, respectively. ^{23}Na spin-lattice (T_1) relaxation times were measured for the heparin/Na^+ and heparin/Na^+/M^{n+} systems over a range of solution conditions to characterize the relaxation properties of heparin-bound Na^+ and its displacement from the counterion condensation volume by M^{n+}. ^1H–^1H nuclear Overhauser enhancements (NOEs) were measured to characterize conformational changes which result from metal binding to heparin.

2. Experimental

Materials.—Beef lung heparin (sodium salt) (153 USP units/mg, 16,000–17,000 molecular weight) and beef intestinal mucosal heparin (sodium salt) 172 USP units/mg, 10,000–12,000 molecular weight) were obtained from Sigma Chemical Co. Reagent grade NaCl, $CaCl_2 \cdot 2H_2O$ and $ZnCl_2 \cdot 2H_2O$ were obtained from Fisher Scientific Co., $MgCl_2 \cdot 6H_2O$ from Mallinckrodt Chemical Co. and $LaCl_3 \cdot 7H_2O$ from Sigma Chemical Co. For the ^1H NMR studies, solutions of the di- and tri-valent metal ions were prepared in 99.8 atom% D_2O (Icon Services, Summit, New Jersey); concentrations were determined by EDTA titration [44].

Heparin characterization.—Concentrated heparin solutions were dialyzed using Spectrapor membrane tubing (3.5 kD cutoff) for several hours against running, distilled water to remove small molecule impurities. Dialysates were adjusted to neutral pH and lyophilized. The lyophilized material was then dissolved in D_2O to give stock solutions ~ 10 mM in the sodium form of the heparin repeating disaccharide unit. ^1H NMR measurements were used to confirm sample integrity and to quantitate the extent of substitution of the acetamido group for the 2-sulfamino group of the A ring. Sulfate and carboxylate groups were quantitated by conductimetric titration [45]. The procedure involved conversion of sodium heparinate to heparinic acid by passing it through an Amberlite IR-120 (Aldrich Chemical Co.) ion-exchange column in the H^+ form, followed by titration with standard base. Solution conductance was measured with a YSI

Model 35 meter and Model 3404 dip cell (YSI, Yellow Springs, Ohio). After determining the total number of anionic sites on the polymer, NaCl was added to give heparin stock solutions having a total sodium ion concentration of 0.15 M for the ^{1}H NMR studies of metal binding.

Sample preparation.—NMR measurements were made on D_2O or 90% H_2O–10% D_2O solutions containing heparin, metal salt and NaCl. Heparin concentrations are expressed in terms of the repeating disaccharide unit. For the ^{1}H NMR studies, aliquots of metal ion and heparin solutions were added to NMR tubes to yield total sample volumes of 0.75 mL and metal ion to carboxylate ratios of $\sim$ 1:1 and 2:1. A small amount of 2,2-dimethyl-2-silapentane-5-sulfonate (DSS, Aldrich) was added for a chemical shift reference. Tubes were immersed in a circulating water bath thermostatted at 37°C, and sample pH was measured using an Orion Model 701A digital ion analyzer equipped with an Ingold combination glass membrane pH electrode that was calibrated at 37°C using certified standard buffer solutions. pH meter readings for D_2O solutions were converted to pD using the equation $pD = pH_{\text{meter reading}} + 0.4$ [46]. Sample pD was adjusted using concentrated DCl and NaOD.

For the ^{23}Na NMR studies, solutions were prepared in 90% H_2O–10% D_2O from weighed amounts of heparin, di- or tri-valent metal salt and NaCl. Solution pH was measured at 25°C, and the pH was adjusted with concentrated HCl and NaOH. In the NaCl titration experiments, aliquots of stock NaCl solution were added to the solution in the NMR tube.

NMR measurements.—^{1}H NMR spectra were measured at 500 MHz with a Varian VXR-500S spectrometer. Chemical shifts are reported vs. the DSS reference signal. All measurements were made at 37°C with presaturation of the HOD signal at 4.64 ppm. ^{1}H chemical shift titrations were carried out over the pD range 1–9, with spectra measured at 10–30 pD values per titration. Two-dimensional nuclear Overhauser effect (NOESY) spectra were measured with a mixing time of 0.075 s; it was determined previously that NOESY cross peaks are in the initial rate regime at this mixing time [47,48]. NOESY spectra were acquired at 37°C using a relaxation delay of 2.8 s ($\sim 2 \times T_1$), including 1.1 s for HOD presaturation. A spectral width of 2600 Hz was used in $F1$ and $F2$, and 2K data points were collected in $F2$ at 128 t_1 increments. A total of 64 transients were coadded for each t_1 increment. The data were processed with zero-filling to 2048 points in $F1$, and apodized with shifted sine bell squared functions in both $F1$ and $F2$. ^{23}Na NMR spectra were measured at 52.9 MHz and 25°C with a Varian XL-200 spectrometer. Samples were contained in 10 mm NMR tubes. ^{23}Na spin-lattice (T_1) and spin–spin (T_2) relaxation times were measured with inversion–recovery and Carr–Purcell–Meiboom–Gill (CPMG) pulse sequences, respectively. Relaxation delays of at least $20T_1$ were used in all relaxation time measurements, and spectra were measured at 10–20 different longitudinal or transverse relaxation periods in the T_1 and T_2 determinations, respectively. T_1 values were determined by a three-parameter (I_o, A and T_1) fit of the inversion–recovery data to the equation:

$$I_t = I_o(1 - Ae^{-t/T_1}). \quad (1)$$

T_2 values were determined by a two-parameter (I_o and T_2) fit to the equation:

$$I_t = I_o e^{-t/T_2}. \quad (2)$$

T_1 and T_2 were found to be equal, indicating $\omega\ \tau_c \ll 1$ (the extreme narrowing condition), where ω and τ_c are the ^{23}Na NMR frequency and correlation time, respectively [27].

3. Results

Heparin.—Bovine lung and intestinal mucosal heparin were characterized as described in the Experimental section. The average charge/disaccharide unit was found by conductometric titration to be 3.68 and 3.52 for lung and intestinal mucosal heparin, respectively. The acetamido content was found by ^{1}H NMR spectroscopy to be 3.8% and 13.7% for lung and intestinal mucosal heparin, respectively. Because the 2-sulfamino group is reported to be involved in Ca^{2+} binding [20], bovine lung heparin was used in most of the metal ion binding studies reported here.

The 500 MHz ^{1}H NMR spectrum of 10 mM bovine lung heparin (pD 7.4, 0.15 M total Na^+) is shown in Fig. 1. Also shown is the heparin repeating disaccharide, with the I and A rings in the $^1C_4$ and $^4C_1$ conformations, respectively. The assignments given for

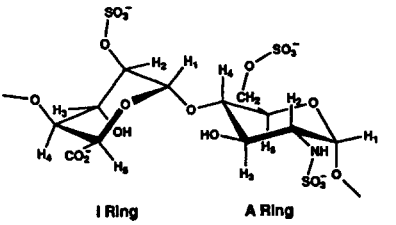

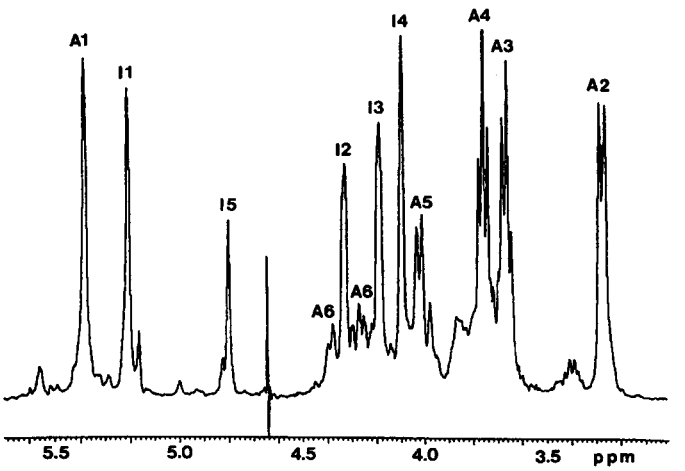

Fig. 1. 500 MHz ^{1}H NMR spectrum of 10 mM sodium heparinate in D_2O at pD 7.4, 37°C and 0.15 M total Na^+. The HOD resonance was suppressed by presaturation. The heparin disaccharide repeating unit is shown with the I and A rings in the $^1C_4$ and $^4C_1$ conformations, respectively.

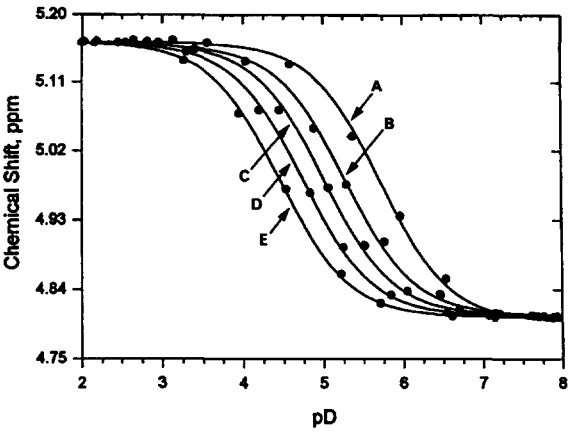

Fig. 2. Chemical shift titration data for the I-5 resonance of heparin (0.002 M) as a function of total Na^+ concentration. Data sets A–E: 0.011, 0.025, 0.050, 0.100 and 0.200 M total Na^+ respectively, D_2O solution at 37°C. The curves through the points are theoretical curves predicted by the pK_a values determined from nonlinear least-squares fits.

the major resonances in Fig. 1 are from Holme and Perlin [49]. Not shown are the *N*-acetyl methyl resonance for the acetamido group and other minor resonances near 2.00 ppm.

The acid–base chemistry of the carboxylic acid group of heparin was characterized by measuring ^1H NMR spectra as a function of pD. Fig. 2 shows the pD dependence of the I-5 resonance for 2 mM heparin in D_2O solutions containing 11, 25, 50, 100, and 200 mM total Na^+. The I-5 resonance shifts upfield by 0.372 ppm over the pD range 2–6 as the carboxylic acid group is titrated. The acid dissociation constant for the carboxylic acid group was determined at each Na^+ concentration by fitting the chemical shift titration curves to eq (3):

$$\delta_o = \frac{K_a\delta_A + [D_3O^+]\,\delta_{HA}}{K_a + [D_3O^+]} \tag{3}$$

where δ_o is the observed chemical shift for the I-5 resonance and δ_{HA} and δ_A the chemical shifts of the I-5 resonance for the carboxylic acid and carboxylate forms of heparin. The results are reported in Table 1. The solid curves through the experimental points in Fig. 2 are theoretical curves calculated with the pK_a values in Table 1. Also reported in Table 1 are pK_a values determined for 10 mM bovine lung and intestinal mucosal heparin in 0.15 M NaCl–D_2O solution.

The acid–base chemistry of heparin was also studied by measuring ^{23}Na spin-lattice (T_1) relaxation times as a function of solution conditions. ^{23}Na spin-lattice relaxation times, which depend on the magnitudes and rates of fluctuations of local electric field gradients at the ^{23}Na nucleus, change upon binding to heparin [27,41]. T_1 and T_2 data could be fit by single exponential functions, which indicates that exchange of Na^+ between its free and heparin-bound forms is fast [27], in which case the observed T_1 values can be treated in terms of a two-site (free and bound) exchange-averaged model

Table 1
Acid-dissociation constants for heparin [a,b]

$[Na^+]_t$ (M)	[Heparin] (M)	pK_a [c]
0.011	0.002	5.71
0.025	0.002	5.26
0.050	0.002	4.99
0.100	0.002	4.73
0.200	0.002	4.45
0.150	0.010	4.70
0.150	0.010	4.69

[a] Conditions: 37°C, D_2O solution.
[b] Bovine lung heparin except last entry which is for bovine intestinal mucosal heparin.
[c] The standard deviation is ± 0.02 pK_a units.

[27,41,50]. The exchange-averaged T_1s are population-weighted averages of the T_1s for the free and bound forms:

$$\frac{1}{T_{1o}} = \frac{P_f}{T_{1f}} + \frac{P_b}{T_{1b}} \tag{4}$$

where T_{1o} is the observed T_1 and T_{1f} and T_{1b} the T_1s and P_f and P_b the molar fractions of Na^+ in the free and bound forms. Substitution of $P_f = 1 - P_b$ into eq (4) leads to:

$$\frac{1}{T_{1o}} = P_b\left(\frac{1}{T_{1b}} - \frac{1}{T_{1f}}\right) + \frac{1}{T_{1f}}. \tag{5}$$

P_b is equal to $[Na^+]_b/[Na^+]_t$, where $[Na^+]_b$ and $[Na^+]_t$ are the concentrations of bound and total Na^+. $[Na^+]_b$ is equal to $\theta_{Na}A$, where θ_{Na} is the fraction of heparin anionic charges neutralized by bound Na^+ and A is the concentration of heparin anionic sites ($= N \times$ [Heparin] where N is the number of anionic sites/disaccharide). Substitution into eq (5) gives:

$$\frac{1}{T_{1o}} = \frac{\theta_{Na}A}{[Na^+]_t}\left(\frac{1}{T_{1b}} - \frac{1}{T_{1f}}\right) + \frac{1}{T_{1f}}. \tag{6}$$

θ_{Na} is a constant, determined by the linear charge density on heparin.

If the two-site model is valid, eq (6) predicts that $1/T_{1o}$ will be a linear function of $A/[Na^+]_t$. To determine if this is the case, T_1 values were measured for solutions containing 0.002 M heparin and $[Na^+]_t$ ranging from 0.007 to 0.2 M. The results are plotted according to eq (6) in Fig. 3. The plot is linear with a slope of 144.5 and an intercept of 19.2 s^{-1}, which confirms the validity of the two-site model for analysis of the ^{23}Na T_1 data.

In Fig. 4 are plotted ^{23}Na T_1 values as a function of pH for solutions containing 0.002 M heparin plus 0.0093 M total Na^+ (curve A) or 0.050 M total Na^+ (curve B). Over this pH range, Na^+ is present in three forms: free, bound to the CO_2H form of heparin and bound to the CO_2^- form of heparin. The decrease in T_1 as the pH is increased from 2 to 6 reflects the increased binding of Na^+ as the carboxylic acid group

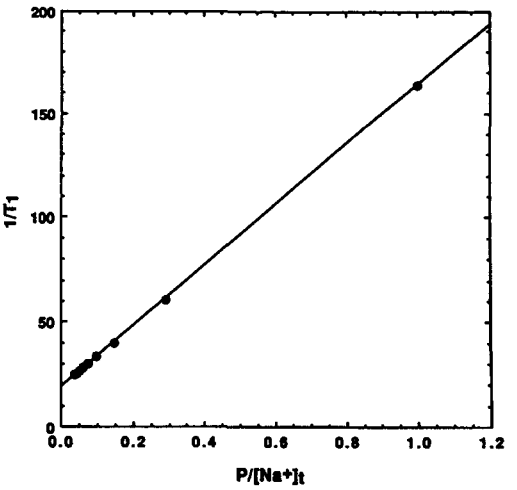

Fig. 3. Plot of $1/T_1$ (^{23}Na) vs. $P/[Na^+]_t$ for a solution containing 0.002 M heparin as a function of the total Na^+ concentration at 25°C. The solvent was 90% H_2O–10% D_2O and the solution pH was in the range 5.7–6.1. P is the concentration of heparin anionic sites.

is titrated and a different T_1 for bound Na^+. The observed T_1 is given by eq (7):

$$\frac{1}{T_{1o}} = \frac{P_f}{T_{1f}} + \frac{P_b^{CO_2H}}{T_{1b}^{CO_2H}} + \frac{P_b^{CO_2^-}}{T_{1b}^{CO_2^-}} \tag{7}$$

where $P_b^{CO_2H}$ and $P_b^{CO_2^-}$ are the molar fractions of Na^+ bound to the CO_2H and CO_2^-

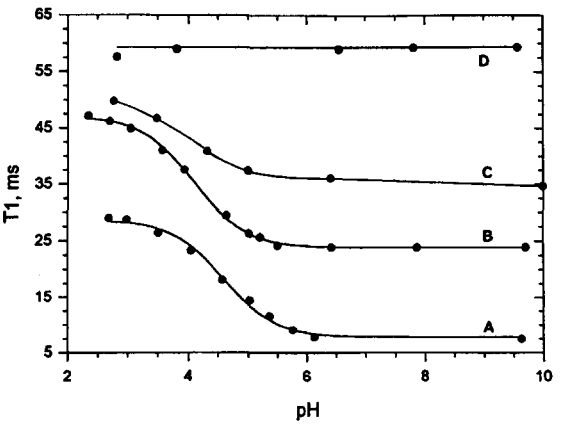

Fig. 4. ^{23}Na T_1 values as a function of pH for (A) 0.002 M heparin, 0.093 M total Na^+, (B) 0.002 M heparin, 0.050 M total Na^+, (C) 0.002 M heparin, 0.002 M Ca^{2+}, 0.050 M total Na^+ and (D) 0.050 M Na^+. In 90% H_2O–10% D_2O solution at 25°C. The curves through data sets A and B are theoretical curves predicted using parameters obtained from nonlinear least-squares fits. The curves through data sets C and D were drawn to connect the data points.

forms of heparin. $P_b^{CO_2H} = \alpha_o \theta_{Na}^{CO_2H} N^{CO_2H}[\text{Heparin}]/[Na^+]_t$ and $P_b^{CO_2^-} = \alpha_1 \theta_{Na}^{CO_2^-} N^{CO_2^-}[\text{Heparin}]/[Na^+]_t$ where $\theta_{Na}^{CO_2H}$ and $\theta_{Na}^{CO_2^-}$ are the fraction of anionic sites neutralized by Na^+ in the CO_2H and CO_2^- forms of heparin, N^{CO_2H} and $N^{CO_2^-}$ are the number of anionic sites/heparin disaccharide for the CO_2H and CO_2^- forms of heparin, and $\alpha_o (= [H^+]/([H^+] + K_a)$ where K_a is the acid dissociation constant for the carboxylic acid group) and $\alpha_1 (= K_a/([H^+] + K_a))$ are the fractions of heparin in the CO_2H and CO_2^- forms. Substitution of the relationship $P_f = 1 - P_b^{CO_2H} - P_b^{CO_2^-}$ and the above definitions for $P_b^{CO_2H}$ and $P_b^{CO_2^-}$ into eq (7) yields:

$$\frac{1}{T_{1o}} = \frac{1}{T_{1f}} + \frac{\alpha_o N^{CO_2H} \theta_{Na}^{CO_2H}[\text{Heparin}]}{[Na^+]_t}\left(\frac{1}{T_{1b}^{CO_2H}} - \frac{1}{T_{1f}}\right) + \frac{\alpha_o N^{CO_2^-} \theta_{Na}^{CO_2^-}[\text{Heparin}]}{[Na^+]_t}\left(\frac{1}{T_{1b}^{CO_2^-}} - \frac{1}{T_{1f}}\right). \quad (8)$$

The data plotted as curves A and B in Fig. 4 were fit by nonlinear least-squares methods to eq (8) to determine K_a, $T_{1b}^{CO_2H}$ and $T_{1b}^{CO_2^-}$. The value used for T_{1f} (0.0556 s) was obtained from the T_1 data for 0.050 M NaCl (plotted as curve D in Fig. 4). The values used for $\theta_{Na}^{CO_2^-}$ (0.59) and $\theta_{Na}^{CO_2H}$ (0.43) were estimated using the counterion condensation model. In the counterion condensation model, the number of delocalized monovalent counterions per fixed polyelectrolyte charge, θ_1, is given by eq (9):

$$\theta_1 = 1 - \xi^{-1} \quad (9)$$

where $\xi = (7.1/b)$ for water at 25°C and b is the average axial charge spacing in Å [43]. Taking the length of a heparin tetrasaccharide unit to be 20.4 Å [38], b is estimated to be 2.9 and 4.1 Å for the carboxylate and low pH carboxylic acid forms of heparin having, on average, seven acidic groups per tetrasaccharide segment. Using these values

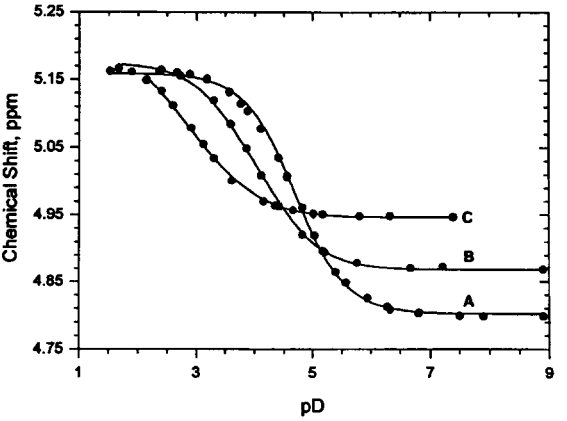

Fig. 5. Chemical shift titration data for the I-5 resonance of 0.010 M heparin, 0.150 M total Na^+ (A); 0.010 M heparin, 0.010 M Ca^{2+} and 0.150 M total Na^+ (B); and 0.010 M heparin, 0.0126 M La^{3+} and 0.150 M total Na^+ (C) in D_2O at 37°C. The curves drawn through the data sets are theoretical curves predicted by parameters from the nonlinear least-squares fits.

for b, ξ is calculated to be 2.45 and 1.73 and θ_{Na} to be 0.59 and 0.43 for the carboxylate and carboxylic acid forms of heparin.

The results obtained from the fit of the 0.0093 M $[Na^+]_t$ data (data set A in Fig. 4) are $pK_a = 5.16 \pm 0.07$, $T_{1b}^{CO_2H} = 0.0116 \pm 0.0003$ s, and $T_{1b}^{CO_2^-} = 0.00394 \pm 0.0003$ s. For the 0.050 M $[Na^+]_t$ data (B in Fig. 4), $pK_a = 4.38 \pm 0.01$, $T_{1b}^{CO_2H} = 0.01134 \pm 0.0003$ s, and $T_{1b}^{CO_2^-} = 0.00340 \pm 0.00004$ s. The solid curves through data sets A and B in Fig. 4 are theoretical curves predicted by eq (8) with the parameters determined from the nonlinear least-squares analysis.

Using the average of these two values for $T_{1b}^{CO_2^-}$ and the value from the intercept in Fig. 3 (19.2 s^{-1}) for $1/T_{1f}$, a value of 0.58 is calculated for $\theta_{Na}^{CO_2^-}$ from the slope of the plot in Fig. 3, in excellent agreement with the value of 0.59 predicted by counterion condensation theory and the value of 0.63 determined experimentally [37].

Heparin–metal binding.—Chemical shift vs. pD data are plotted in Fig. 5 for the I-5 resonance of heparin in solutions containing 0.010 M heparin and 0.150 M total Na^+ (curve A) and 0.010 M heparin, 0.150 M total Na^+ and 0.010 M Ca^{2+} (curve B) or 0.0126 M La^{3+} (curve C). The I-5 chemical shift titration curve is shifted to lower pD in the presence of Ca^{2+} and La^{3+}, corresponding to an apparent increase in the acidity of the carboxylic acid group, and the high pH chemical shifts are different, both of which indicate binding of Ca^{2+} and La^{3+} by heparin.

Binding constants, (defined by eqs (10) and (11)) were determined from the heparin/Na^+/M^{n+} chemical shift titration curves by fitting the data to eq (12) by nonlinear least squares methods:

$$M^{n+} + \text{Heparin} \rightleftharpoons M^{n+} - \text{Heparin} \tag{10}$$

$$K_b = \frac{[M^{n+} - \text{Heparin}]}{[M^{n+}][\text{Heparin}]} \tag{11}$$

where [Heparin] is the concentration of the heparin repeating disaccharide unit.

$$\delta_o = P_f \delta_f + P_b \delta_b. \tag{12}$$

P_f and P_b are the molar fractions of heparin in the free and bound forms, δ_f the

Table 2
Metal–heparin binding constants [a,b]

M^{n+}	M^{n+}/CO_2^-	δ_b(ppm)	$\log K_b$ [c]
Ca^{2+}	0.99	4.902	2.65
Ca^{2+}	1.01	4.903	2.64
Ca^{2+}	2.02	4.900	2.53
Mg^{2+}	1.02	4.835	2.08
Mg^{2+}	2.03	4.843	1.99
Zn^{2+}	1.03	4.916	2.68
Zn^{2+}	2.05	4.925	2.59
La^{3+}	1.26	4.952	3.56

[a] Conditions: 37°C, 0.150 M total Na^+, ca. 0.010 M heparin carboxylate group, D_2O solution.
[b] Bovine lung heparin except first entry which is for bovine intestinal mucosal heparin.
[c] Standard deviation is ± 0.03 $\log K_b$ units.

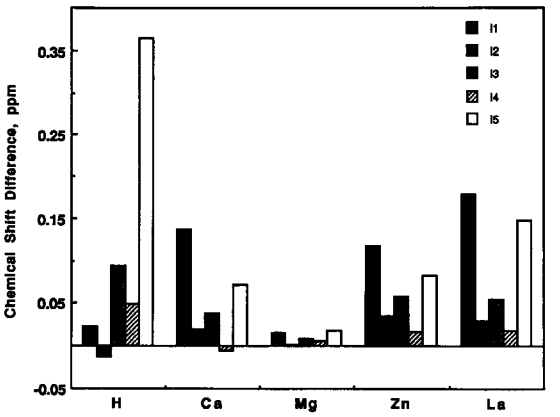

Fig. 6. Changes in the chemical shifts of the I ring resonances of the carboxylate form of sodium heparinate in D_2O solution (0.010 M heparin, 0.010 M M^{n+} and 0.150 M total Na^+ at neutral pD) upon protonation of the carboxylate group (H) and binding of Ca^{2+}, Mg^{2+}, Zn^{2+} and La^{3+}. Positive differences indicate downfield shifts. The chemical shifts of the I ring resonances of the carboxylate form of heparin at neutral pD are (±0.004 ppm): I-1, 5.208; I-2, 4.328; I-3, 4.188; I-4, 4.091 and I-5, 4.802 ppm.

chemical shift of the I-5 resonance of free heparin at the pD at which δ_0 was measured, and δ_b the chemical shift of the bound heparin. In the nonlinear least squares fitting procedure, P_f and P_b were expressed in terms of K_b. The binding constants are reported in Table 2. The solid lines through the experimental points in Fig. 5 are theoretical curves predicted using the pK_a value for the carboxylic acid group (curve A) and the Ca^{2+}–heparin (curve B) and La^{3+}–heparin (curve C) binding constants. The changes in chemical shift of the I ring and A ring resonances of sodium heparinate caused by protonation of the carboxylate group and by binding of Mg^{2+}, Ca^{2+}, Zn^{2+} and La^{3+} are presented in Figs. 6 and 7, respectively.

Binding of M^{2+} by heparin is accompanied by the release of about 2 Na^+ [17]:

$$M^{2+}(\text{free}) + 2\,Na^+(\text{bound}) \rightleftharpoons 2\,Na^+(\text{free}) + M^{2+}(\text{bound}). \quad (13)$$

Displacement of Na^+ from heparin by Ca^{2+}, Mg^{2+} and Zn^{2+} was studied by ^{23}Na NMR. Data set C in Fig. 4 is the T_1 measured as a function of pH for a solution containing 0.002 M heparin, 0.002 M Ca^{2+} and 0.050 M total Na^+. The observed T_1 values lie between those for 0.002 M heparin–0.050 M total Na^+ (curve B) and 0.050 M Na^+ (curve D), consistent with displacement of bound Na^+ by Ca^{2+} (eq (13)). Equilibrium constants for the ion-exchange reaction in eq (13), K_{ex}, for Ca^{2+} Mg^{2+} and Zn^{2+} were estimated from exchange-averaged ^{23}Na T_1 values measured for heparin/Na^+/M^{2+} solutions as a function of the Na^+ concentration. The exchange constant is defined by eq (14).

$$K_{ex} = \frac{(M^{2+})_b(Na^+)_f^2}{(M^{2+})_f(Na^+)_b^2}. \quad (14)$$

Data set A in Fig. 8 is for a solution containing 0.002 M heparin and total Na^+ up to

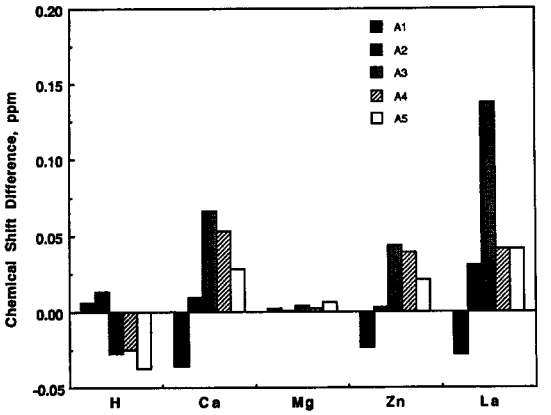

Fig. 7. Changes in the chemical shifts of the A ring resonances of heparin upon protonation of the carboxylate group (H) and binding of Ca^{2+}, Mg^{2+}, Zn^{2+} and La^{3+} to the carboxylate form of heparin. Conditions are given in the legend to Fig. 7. The chemical shifts of the A ring resonances of the carboxylate form of heparin at neutral pD (±0.004 ppm): A-1, 5.384; A-2, 3.269; A-3, 3.657; A-4, 3.755 and A-5, 4.017 ppm.

0.020 M. Data sets B, C and D are for solutions which also contained 0.002 M Ca^{2+}, Mg^{2+}, or Zn^{2+} respectively. Data set E is for the heparin/Na^+/La^{3+} system. Calculation of K_{ex} for the Ca^{2+}, Mg^{2+}, and Zn^{2+} systems involved first calculation of the mole fraction of bound Na^+ with eq (15), which was obtained by rearrangement of eq (5).

$$P_b = \frac{T_{1b}(T_{1f} - T_{1o})}{T_{1o}(T_{1f} - T_{1b})}. \tag{15}$$

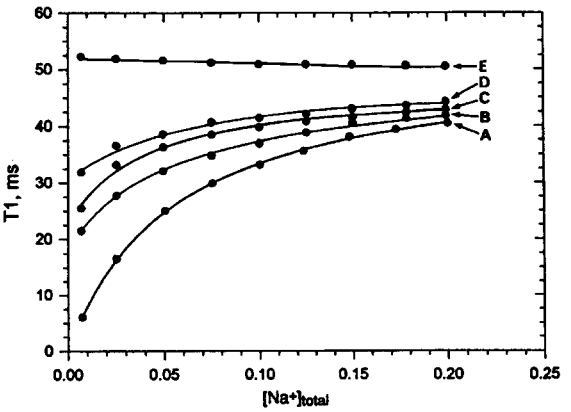

Fig. 8. T_1 values for ^{23}Na in solutions containing 0.002 M heparin (A) and 0.002 M heparin with 0.002 M Mg^{2+} (B), Ca^{2+} (C) and Zn^{2+} (D) and 0.0025 M La^{3+} (E) as a function of the total Na^+ concentration at 25°C. Solvent was 90% H_2O–10%D_2O and solution pH was in the range 5.7–6.1. The curve through data set A is the theoretical curve predicted by parameters from the nonlinear least-squares fit. The curves through the other data sets were drawn to connect data points.

Table 3
M^{2+}–Na^+ Exchange equilibrium constants [a]

M^{2+}	$\log K_{ex}$
Ca^{2+}	3.3±0.1
Mg^{2+}	2.6±0.1
Zn^{2+}	3.6±0.1

[a] Conditions: 25°C, 90% H_2O–10% D_2O solution, total Na^+ varied from 0.007 to 0.2 M.

The T_1 for 0.050 M NaCl was used for T_{1f} and the value used for T_{1b} was obtained from the fit of the data in curve B in Fig. 4. The concentration of bound Na^+ was calculated using this value for $P_b([Na^+]_b = P_b[Na^+]_t)$; the concentrations of the other species were then calculated using $[Na^+]_b$ and the stoichiometry of the exchange reaction (eq (13)). The values calculated for K_{ex} are constant over the Na^+ concentration range in Fig. 8 and are reported in Table 3.

Conformational studies.—NOESY spectra were measured for the CO_2H and CO_2^- forms of heparin in solutions which contained 0.010 M heparin and 0.150 M total Na^+, and in solutions which contained approximately equimolar concentrations of heparin and M^{n+} (0.010 M) and 0.15 M total Na^+. A representative NOESY spectrum measured for the heparin/Na^+/Ca^{2+} system at pD 8.0 is presented in Fig. 9. NOE cross-peak intensities are reported in Table 4.

4. Discussion

Sodium heparinate behaves as a polyelectrolyte, with a fraction of its negative charge neutralized by Na^+, which is closely associated with the polyanionic polymer. Accord-

Table 4
^1H–^1H NOE values for selected heparin resonances in heparin–Na^+–M^{n+} systems [a]

Cation(s)	pD	NOE Intensity ratios [b,c]					
		A-1–*A-2*	A-1–*I-4*	A-1–*I-3*	I-1–*A-4*	I-1–*I-2*	I-5–*I-4*
Na^+	2.4	13.4	11.2	5.7	3.9	5.7	6.2
Na^+–Mg^{2+}	2.6	13.7	11.0	4.6*	3.4	5.8	6.4
Na^+–Ca^{2+}	2.4	13.3	11.0	5.8	3.8	6.3	6.1
Na^+	7.4	13.9	8.4	7.2*	3.8	5.4	3.4
Na^+–Mg^{2+}	7.3	13.8	7.8	7.0	3.8	4.5	3.1
Na^+–Ca^{2+}	8.0	13.3	9.9	8.1	5.3	9.0	5.6
Na^+–La^{3+}	7.2	12.8	8.6	6.1	4.6	6.8	6.6

[a] Conditions: 0.010 M bovine lung heparin and M^{n+}; 0.15 M total Na^+ in D_2O at 37°C.
[b] NOE ratios are defined as crosspeak volume/diagonal volume ×100%. Crosspeaks are between proton pairs as designated, with the diagonal element given in italics.
[c] Averages from three separate NOESY spectra measured with a mixing time of 0.075 s. The average standard deviation for NOE ratios is ±0.4; those with somewhat larger standard deviations are indicated with an asterisk.

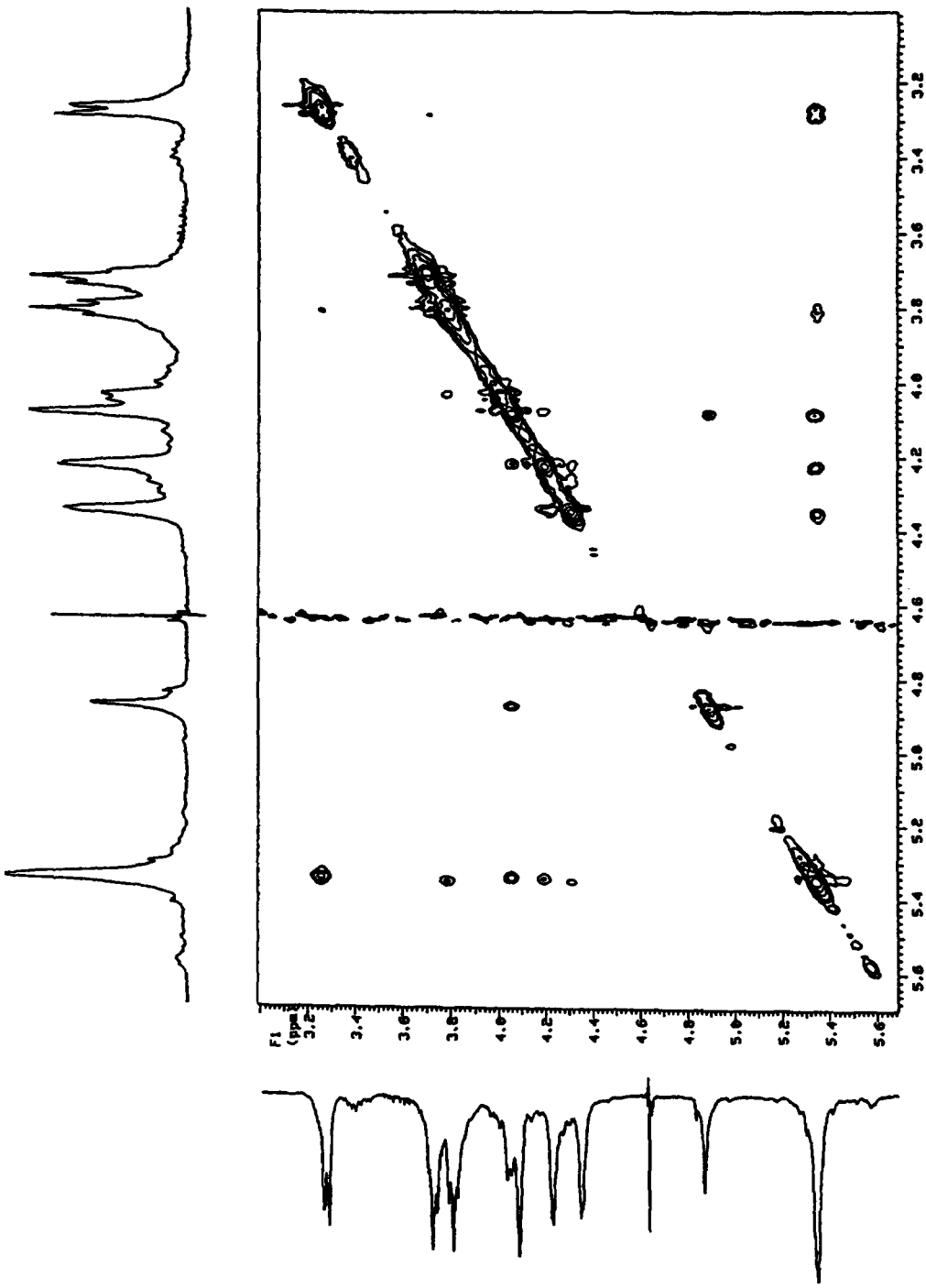

Fig. 9. Two-dimensional NOESY spectrum of a pD 8.0 D_2O solution containing 0.010 M heparin, 0.010 M Ca^{2+} and 0.150 M total Na^+. The HOD resonance was suppressed by presaturation and a mixing time of 0.075 s was used. The one-dimensional spectrum is plotted along the top and side.

ing to counterion condensation theory, the extent of Na^+ binding by heparin depends on the axial charge density and is invariant to the molarity of Na^+ in free solution [42,43]. The linearity of the plot in Fig. 3 indicates that $\theta_{Na}^{CO_2^-}$ is constant up to 0.2 M total Na^+.

The chemical shift titration curves in Fig. 2 and the pK_a values in Table 1 indicate a strong dependence of the acidity of the heparin carboxylic acid group on the molarity of Na^+ in free solution. The pK_a values reported in Table 1 are mixed equilibrium constants, expressed in terms of the activity of H^+ and the concentration of the CO_2H and CO_2^- forms of heparin. Debye–Hückel theory predicts that K_a will increase as the Na^+ concentration, and thus the ionic strength, increases. For the Na^+ concentration range in Fig. 2 and Table 1, an increase in acidity corresponding to a decrease in pK_a of < 0.5 units is predicted. The larger decrease in pK_a is due to the polyelectrolyte character of heparin. Titration of the carboxylic acid group causes an increase in axial charge density, which in turn causes θ_{Na} to increase from 0.43 to 0.59 and the concentration of Na^+ in the counterion condensation volume, C_{Na}^{loc}, to increase. In the counterion condensation model, the delocalized bound counterions are contained in a volume V_p surrounding the polyelectrolyte [43]. V_p depends on the axial charge spacing as given by eq (16):

$$V_p = 41.1(\xi - 1)b^3 \tag{16}$$

where V_p has the units cm^3/mol of polyelectrolyte charge. The concentration of delocalized monovalent counterion in the condensation volume surrounding the polyelectrolyte, C_1^{loc}, is given by eq (17):

$$C_1^{loc} = 10^3\theta_1 V_p^{-1} = 24.3(\xi b^3)^{-1}. \tag{17}$$

Using the theoretical value of 0.43 for $\theta_{Na}^{CO_2H}$ and the experimental value of 0.63 for $\theta_{Na}^{CO_2^-}$, C_{Na}^{loc} is estimated to be 0.21 and 0.41 M for the CO_2H and CO_2^- forms of heparin, i.e., there is a net transfer of Na^+ from free solution to the counterion condensation volume around heparin as the carboxylic acid group is titrated. This is entropically unfavored if the concentration of free Na^+, C_{Na}, is less than C_{Na}^{loc}. Thus, pK_a is predicted to increase as C_{Na} is decreased. It is also of interest to note that, at constant $[Na^+]_t$, the pK_a depends on the heparin concentration since C_{Na} decreases as the heparin concentration increases. To illustrate, the pK_a of 0.010 M heparin in 0.150 M $[Na^+]_t$ is similar to the pK_a of 0.002 M heparin in 0.100 M $[Na^+]_t$ (Table 1).

The binding constants in Table 2 together with the chemical shift data in Figs 6 and 7 suggest that the nature of Mg^{2+}–heparin binding is different from Ca^{2+}, Zn^{2+} and La^{3+}–heparin binding. Release of Na^+ by the exchange reaction in eq (13) provides an entropic driving force for the binding of M^{n+} where $n > 1$ [17,35]. If the binding of Mg^{2+}, Ca^{2+} and Zn^{2+} was completely delocalized with only entropic contributions determining the binding constants, they would be the same for all three cations. This is not the case, which suggests some site-specific binding [17,18].

Protonation of the carboxylate group, which is site specific, causes large changes in the chemical shifts of I ring resonances (Fig. 6) due to through-bond inductive effects, and smaller but significant changes in the chemical shifts of some of the A ring resonances (Fig. 7) due to changes in conformation across the ($GlcNSO_3$-6S)-(1 → 4)-

(IdoA-2S) glycosidic bond [47]. Binding of Ca^{2+}, Zn^{2+} and La^{3+} by heparin also causes large changes in heparin chemical shifts, whereas changes caused by binding of Mg^{2+} are relatively small. These results suggest that binding of Mg^{2+} is similar to that of the Na^+ it replaces, i.e., delocalized, whereas binding of Ca^{2+}, Zn^{2+} and La^{3+} involves site-specific interactions, at least part of the time, presumably with the carboxylate and sulfamino groups. Thus, changes in chemical shift in the presence of Ca^{2+}, Zn^{2+} and La^{3+} result from a combination of through-bond inductive effects and changes in conformation induced by site-specific binding, as discussed below. The binding constant for the La^{3+}–heparin complex is larger than for the M^{2+}–heparin complexes, presumably due to both a larger entropic contribution and a larger site-specific contribution.

The NOE results in Table 4 also provide information about the conformation of heparin and the nature of heparin–metal binding. The NOEs for the heparin–Na^+ and heparin–Na^+–Mg^{2+} systems are similar at pD 7.4, which is consistent with delocalized binding of Mg^{2+} by the CO_2^- form of heparin. For the heparin–Na^+–Ca^{2+} and heparin–Na^+–La^{3+} systems, the I-1–A-4 NOE is larger than for the heparin–Na^+ system, which indicates a change in conformation around the (IdoA-2S)-(1 → 4)-($GlcNSO_3$-6S) glycosidic bond. Molecular models show this is consistent with simultaneous binding of M^{n+} to carboxylate and *N*-sulfate groups on adjacent residues. Also, intraresidue NOEs for the CO_2^- form of heparin suggest a change in the conformation of the I ring upon binding Ca^{2+} and La^{3+}. Ferro et al. concluded that the I ring in heparin–Na^+ exists as a 60:40 mixture of the $^1C_4$ and $^2S_0$ conformations, whereas the I ring of the heparin–Na^+–Ca^{2+} system exists as an 80:20 mixture of these two conformations [51]. The increase in the I-1–I-2 and I-5–I-4 NOEs upon binding Ca^{2+} and La^{3+} is consistent with an increased population of the $^1C_4$ conformation.

The difference between the ^{23}Na T_1 for the heparin–Na^+ and heparin–Na^+–Ca^{2+} systems at low pD (curves B and C in Fig. 4) indicates a small amount of Ca^{2+} binding to the CO_2H form of heparin. However, the NOEs for the heparin–Na^+, heparin–Na^+–Ca^{2+} and heparin–Na^+–Mg^{2+} systems at pD 2.4 are essentially identical, which indicates that the conformation of heparin is the same in all three systems. The identical NOEs for the three systems suggest delocalized binding of Ca^{2+} and Mg^{2+} by the CO_2H form of heparin. The chemical shifts of the ^1H resonances of heparin, heparin–Ca^{2+} and heparin–Mg^{2+} are essentially identical at low pH, which also is consistent with delocalized binding of Ca^{2+} and Mg^{2+} by the CO_2H form of heparin.

5. Conclusions

The results presented here, taken together with results from previous studies in which it was found that the 2-sulfamino group of the A-ring is necessary for Ca^{2+} binding whereas the 2-*O*-sulfo group of the I-ring is not [20], and that $\theta_2^{Ca^{2+}}$ and $\theta_2^{Zn^{2+}}$, the fraction of heparin anionic charge neutralized by Ca^{2+} and Zn^{2+}, are both larger than predicted by counterion condensation theory but $\theta_2^{Mg^{2+}}$ is not [17,18], provide strong evidence that the binding of Mg^{2+} by the CO_2^- form of heparin involves delocalized

electrostatic interactions, but that there is a site-specific contribution to the binding of Ca^{2+}, Zn^{2+} and La^{3+}.

Acknowledgement

This research was supported in part by National Institutes of Health Grant AI-24216.

References

[1] W.D. Comper, *Heparin (and Related Polysaccharides)*, Gordon and Breach Science Publishers, New York, 1981.
[2] B. Casu, in D.A. Lane and U. Lindahl (Eds.), *Heparin: Chemical and Biological Properties, Clinical Applications*, CRC Press, Boca Raton, Florida, 1989, pp 25–49.
[3] B. Casu, in S. Dumitriu (Ed.), *Polymeric Biomaterials*, Marcel Dekker, New York, 1994, pp 159–177.
[4] G. Gatti, B. Casu, G.K. Hamer, and A.S. Perlin, *Macromolecules*, 12 (1979) 1001–1007.
[5] B. Casu, *Adv. Carbohydr. Chem.*, 43 (1985) 51–134.
[6] E.W. Salzman, *Ann. N.Y. Acad. Sci.*, 556 (1989) 371–377.
[7] J. Hirsh, *Ann. N.Y. Acad. Sci.*, 556 (1989) 378–385.
[8] V.V. Kakkar and A.R. Hedges, in D.A. Lane and U. Lindahl (Eds.), *Heparin: Chemical and Biological Properties, Clinical Applications*, CRC Press, Boca Raton, Florida, 1989, pp 455–473.
[9] H. Ireland, P.B. Rylance, and P. Kesteven, in D.A. Lane and U. Lindahl (Eds.), *Heparin: Chemical and Biological Properties, Clinical Applications*, CRC Press, Boca Raton, Florida, 1989, pp 549–574.
[10] G. Bengtsson, T. Oivecrona, M. Höök, J. Riesenfeld, and U. Lindahl, *Biochem. J.*, 189 (1980) 625.
[11] E. De Clercq, *Antimicrob. Agents Chemother.*, 23 (1989) 35–46.
[12] D.A. Lane, in D.A. Lane and U. Lindahl (Eds.), *Heparin: Chemical and Biological Properties, Clinical Applications*, CRC Press, Boca Raton, Florida, 1989, pp 363–391.
[13] G. Murano, *Sem. Thromb. Hemostasis*, 6 (1980) 140–162.
[14] S.C. Alter and L.B. Schwartz, *Biochim. Biophys. Acta*, 991 (1989) 426–430.
[15] (a) W.F. Long and F.B. Williamson, *Biochem. Biophys. Res. Commun.*, 104 (1982) 363–368; (b) T.W. Barrowcliffe and Y. LeShirley, *Thromb. Haemostas.*, 62 (1988) 950–954.
[16] T.N. Young, J.M. Edelberg, S. Stack, and S.V. Pizzo, *Arch. Biochem. Biophys.*, 256 (1992) 530–538.
[17] J. Mattai and J.C.T. Kwak, *Biochim. Biophys. Acta*, 677 (1981) 303–310.
[18] J. Mattai and J.C.T. Kwak, *Biophys. Chem.*, 31 (1988) 295–299.
[19] J.J.R. Fraústo da Silva and R.J.P. Williams, *The Biological Chemistry of the Elements*, Clarendon Press, Oxford, 1991, p 223.
[20] L. Ayotte and A.S. Perlin, *Carbohydr. Res.*, 145 (1986) 267–277.
[21] B. Lages and S.S. Stivala, *Biopolymers*, 12 (1973) 127–143.
[22] F. Jooyahdeh, J.S. Moore, G.O. Phillips, and J.V. Davies, *J. Chem. Soc., Perkin Trans. 2*, (1974) 1468–1471.
[23] J. Boyd, F.B. Williamson, and P. Gettins, *J. Mol. Biol.*, 137 (1980) 175–190.
[24] H. Gustavsson, G. Siegel, B. Lindman, and L. Fransson, *Biochim. Biophys. Acta*, 677 (1981) 23–31.
[25] R.F. Parrish and W.R. Fair, *Biochem. J.*, 193 (1981) 407–410.
[26] J.N. Liang, B. Chakrabarti, L. Ayotte, and A.S. Perlin, *Carbohydr. Res.*, 106 (1982) 101–109.
[27] L. Lerner and D.A. Torchia, *J. Biol. Chem.*, 261 (1986) 12706–12714.
[28] N.E. Woodhead, W.F. Long, and F.B. Williamson, *Biochem. J.*, 237 (1986) 281–284.
[29] G.K. Hunter, K.S. Wong, and J.J. Kim, *Arch. Biochim. Biophys.*, 260 (1988) 161–167.
[30] R.N. Rej, K.R. Holme, and A.S. Perlin, *Carbohydr. Res.*, 207 (1990) 143–152.
[31] R.N. Rej, K.R. Holme, and A.S. Perlin, *Can. J. Chem.*, 68 (1990) 1740–1745.
[32] D. Grant, W.F. Long, C.F. Moffat, and F.B. Williamson, *Biochem. J.*, 282 (1992) 601–604.

[33] D. Grant, W.F. Long, and F.B. Williamson, *Biochem. J.*, 285 (1992) 477–480.
[34] Z. Liu and A.S. Perlin, *Carbohydr. Res.*, 236 (1992) 121–133.
[35] P. Dais, Q.-J. Peng, and A.S. Perlin, *Can. J. Chem.*, 65 (1987) 1739–1745.
[36] P. Dais, Q.-J. Peng, and A.S. Perlin, *Carbohydr. Res.*, 168 (1987) 163–179.
[37] F. Ascoli, C. Botre, and A.M. Liquori, *J. Phys. Chem.*, 65 (1961) 1991–1992.
[38] G.P. Diakun, H.E. Edwards, D.J. Wedlock, J.C. Allen, and G.O. Phillips, *Macromolecules*, 11 (1978) 1110–1114.
[39] C. Villiers, C. Braud, and M. Vert, *Carbohydr. Res.*, 83 (1980) 335.
[40] C. Braud, C. Villiers, and M. Vert, *Carbohydr. Res.*, 86 (1980) 165–175.
[41] A. Delville and P. Laszlo, *Biophys. Chem.*, 17 (1983) 119–124.
[42] G.S. Manning, *Acc. Chem. Res.*, 12 (1979) 443–449.
[43] G.S. Manning, *Q. Rev. Biophys.*, 11 (1978) 179–246.
[44] F.J. Welcher, *The Analytical Uses of Ethylenediaminetetraacetic Acid*, Van Nostrand, Princeton, New Jersey, 1958.
[45] B. Casu and U. Gennaro, *Carbohydr. Res.*, 39 (1975) 168–176.
[46] P.K. Glasoe and F.A. Long, *J. Phys. Chem.*, 64 (1972) 188–190.
[47] D.L. Rabenstein, P. Bratt, T.D. Schierling, J.M. Robert, and W. Guo, *J. Am. Chem. Soc.*, 114 (1992) 3278–3285.
[48] D. Neuhaus and M. Williamson, *The Nuclear Overhauser Effect in Structural and Conformational Analysis*, VCH Publishers, New York, 1989.
[49] R.K. Holme and A.S. Perlin, *Carbohydr. Res.*, 186 (1989) 301–312.
[50] C.F. Anderson and M.T. Record, *Ann. Rev. Biophys. Biophys. Chem.*, 19 (1990) 423–465.
[51] D.R. Ferro, A. Provasoli, M. Ragazzi, B. Casu, G. Torri, V. Bossennec, B. Perly, P. Sinaÿ, M. Petitou, and J. Choay, *Carbohydr. Res.*, 195 (1990) 157–167.